Int. J. Solids Structures Vol. 28, No. 9, pp. 1095–1104, 1991
Printed in Great Britain.

0020-7683/91 $3.00+.00

THE EFFECT OF PLASTIC DEFORMATION ON CRACK INITIATION IN FATIGUE

H. FAN, L. M. KEER and T. MURA
Department of Mechanical Engineering and Civil Engineering, Northwestern University, Evanston, IL 60208, U.S.A.

(*Received* 29 *May* 1990; *in revised form* 8 *February* 1991)

Abstract—Qualitative considerations are given in the present paper concerning the effects of localized plastic deformation on the fatigue crack initiation life and stress intensity factor of a micro-crack. The localized plastic zone is modelled as an elliptical inhomogeneity with eigenstrains. With the consideration of this localized plastic deformation, the calculated crack initiation cycle number is greater and the stress intensity factor of a micro-crack lower than those obtained without considering the plastic deformation effect.

NOMENCLATURE

a_1, a_2	semi-axes of plastic zone
c	micro-crack length
C_{ijkl}	elastic moduli
n_1	crack initiation cycle number
τ_Y	yielding stress in shear
τ_f	internal friction stress
ν	Poisson's ratio
μ	elastic shear modulus
μ_p	plastic shear modulus
ε^p	plastic strain
ε^*	eigenstrain.

1. INTRODUCTION

The prediction of fatigue crack initiation has attracted many researchers in both the experimental and theoretical fields of research. Some models have been made to explain the mechanisms of fatigue crack initiation [e.g. Lin *et al.* (1986) and Tanaka and Mura (1981)]. It is recognized that the persistent slip band (PSB) plays an important role in the early stages of damage [see Essman *et al.* (1981) and Laird (1978)]. Recently, a dislocation dipole pileup model for crack initiation, proposed by Mura and Nakasone (1990), provided some qualitative relations between the fatigue cycles to initiate a crack and the material properties, such as the elastic modulus and internal friction force. There appears, however, to be no relation between the fatigue life and the plastic properties of the material. It has been noticed that plastic deformation can be localized in a PSB. Most experimental results show that plastic deformation is needed to produce fatigue failure. On the theoretical side, researchers have also noticed the importance of plastic deformation in crack initiation. Lin and Cheng (1989) treated the plastic zone as slipping layers. Micro-cracking is believed to be initiated in these slip layers.

A next step is the early stage of micro-crack growth, which is believed also to be partly controlled by the local plastic zone. It is well known that crack-tip stresses are shielded by local plastic deformation. Some theoretical models have also been developed to explain this phenomenon. For example, Steif (1987) considered a semi-infinite crack penetrating into a circular inclusion by using the complex variable approach. Further analysis on the structure of the damage zone shows that anisotropic damage can provide the maximal crack-tip shielding [see Ortiz and Giannakopoulos (1989) for a review on this subject]. As another

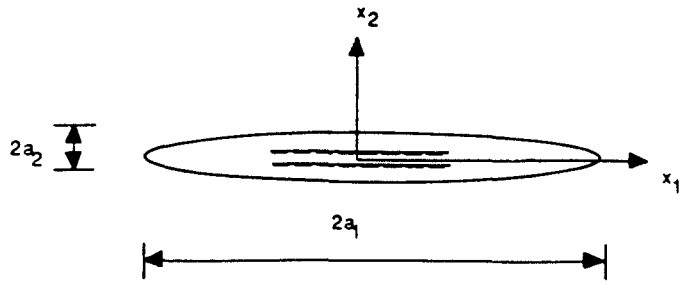

Fig. 1(a). Dislocation dipoles piled up in a plastic zone.

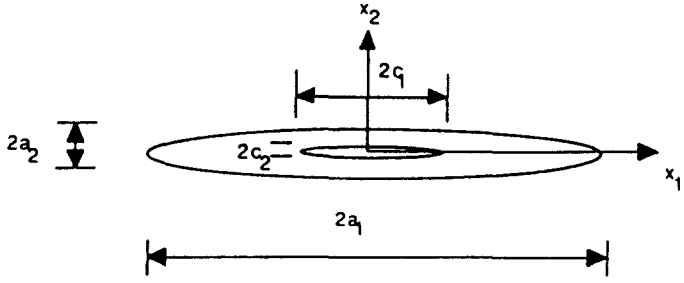

Fig. 1(b). A micro-crack embedded in a plastic zone.

crack shielding example, the interesting configuration [Fig. 1(b)] is considered, where a crack is surrounded by a plastically-deformed zone. It should be pointed out that this plastic deformation is caused by fatigue loading rather than crack-tip stress concentration.

In the present paper, the eigenstrain method is used to model the above two stages of the fatigue life, crack initiation and the early stage of micro-crack propagation. In the first part, the dislocation dipole pileup lines, which are the crack initiation sites, are embedded in a plastic zone. The loading acting at the far field is reduced by the plastic deformation, which delays the crack initiation. Secondly, a micro-crack surrounded by the plastic zone is considered. The crack-tip stress intensity factor is also expected to be reduced. As a qualitative consideration, the persistent slip band is modelled as an elliptically-shaped region with uniform plastic strain. With a calculated stress in the plastic zone, Mura and Nakasone's (1990) fatigue model will be used by replacing their $\Delta\tau$ by $\Delta\tau^p$ to obtain the crack initiation cycle number n_i. In the second part, the crack is also modelled as a smaller elliptical inclusion within the inhomogeneity, and with an eigenstrain that requires the stresses to satisfy the traction-free condition on the crack surface. The stress intensity factor is calculated by considering the stress jump across $\partial\Omega_c$ [see Fig. 1(b)].

2. CRACK INITIATION

Experimental observations show that plastic deformation under fatigue is localized in some slip bands (PSBs), where a PSB in the following is modelled as a narrow elliptically-shaped inclusion. Micro-cracks are believed to be initiated within the band. Mura and Nakasone's (1990) dislocation model is adopted here to describe the crack initiation mechanism. The dislocation pileup lines are assumed to be surrounded by the elliptically-shaped plastic zone, where the plastic strain is assumed to be uniform [see Fig. 1(a)]. Fatigue loading involving plastic deformation is described by Fig. 2. From Hooke's law,

$$\sigma_{ij} = \lambda\delta_{ij}(\varepsilon_{kk} - \varepsilon^p_{kk}) + 2\mu(\varepsilon_{ij} - \varepsilon^p_{ij}).$$

As mentioned before, since slip lines form in a favored direction, only shear deformation along these slip lines is plastic. By using the coordinate shown in Fig. 1(a), a pure shear case is considered hereafter (to avoid too many subscripts, take $\tau = \sigma_{12}$, $\varepsilon = \varepsilon_{12}$):

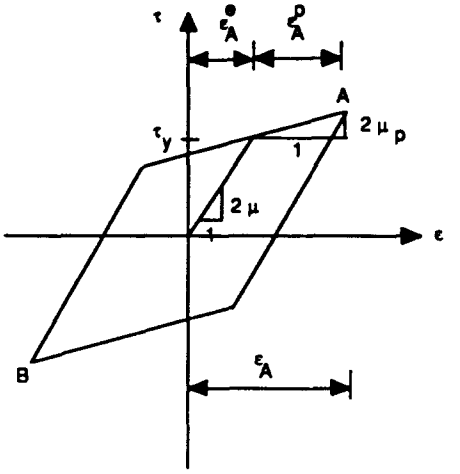

Fig. 2. Hysteresis loop of fatigue.

$$\tau_A = 2\mu(\varepsilon_A - \varepsilon_A^p) \tag{1}$$

where ε_A is the total shear strain and ε_A^p is the plastic part. From the hysteresis loop (Fig. 2), one can write that:

$$\varepsilon_A = \frac{\tau_Y}{2\mu} + \frac{\tau_A - \tau_Y}{2\mu_p} \tag{2}$$

where μ_p is the plastic modulus. In order to simplify the analysis, a stable loop with bi-linear shape is used in the present formulation. Cyclic hardening and softening are not considered. Although the power relation between σ and ε may be closer to reality, a qualitatively similar result to the present analysis is expected.

Substitute eqn (2) into eqn (1)

$$\tau_A = \tau_Y - \frac{2\mu}{(1-\mu/\mu_p)}\varepsilon_A^p. \tag{3}$$

By using the eigenstrain concept (Mura, 1982)

$$\tau_A = \tau_1^\infty + \tau_A^* \tag{4}$$

where τ_1^∞ is the loading at the far field and τ_A^* is caused by the plastic strain. For an isotropic material, it is known from the Eshelby solution (1957) (see Appendix A) that:

$$\tau_A^* = -\frac{2\mu}{(1-\nu)}\frac{a_1 a_2}{(a_1+a_2)^2}\varepsilon_A^p \tag{5}$$

where a_1 and a_2 are the geometrical parameters of this elliptical plastic zone. Equations (3), (4) and (5) lead to:

$$\tau_Y - \frac{2\mu}{(1-\mu/\mu_p)}\varepsilon_A^p = \tau_1^\infty - \frac{2\mu}{(1-\nu)}\frac{a_1 a_2}{(a_1+a_2)^2}\varepsilon_A^p. \tag{6}$$

The eigenstrain ε_A^p is then solved from this equation as:

$$\varepsilon_A^p = \frac{\tau_1^\infty - \tau_Y}{\dfrac{2\mu}{(1-\nu)}\dfrac{a_1 a_2}{(a_1+a_2)^2} - \dfrac{2\mu}{1-\mu/\mu_p}}. \tag{7}$$

Thus,

$$\tau_A = \tau_1^\infty - \frac{2\mu}{(1-\nu)}\frac{a_1 a_2}{(a_1+a_2)^2}\frac{\tau_1^\infty - \tau_Y}{\dfrac{2\mu}{(1-\nu)}\dfrac{a_1 a_2}{(a_1+a_2)^2} - \dfrac{2\mu}{1-\mu/\mu_p}}. \tag{8}$$

When $\mu_p = \mu$, we have $\tau_A = \tau_1^\infty$, and as another limit, $\mu_p = 0$, $\tau_A = \tau_Y$.

Similarly, the stress in the plastic zone at point B (see Fig. 2) can be obtained as:

$$\tau_B = 2\mu(\varepsilon_B - \varepsilon_B^p).$$

Then,

$$\varepsilon_B = -\frac{\tau_Y}{2\mu} + \frac{\tau_2^\infty + \tau_Y}{2\mu_p}$$

which in turn leads to:

$$\tau_B = -\tau_Y - \frac{2\mu}{1-\mu/\mu_p}\varepsilon_B^p. \tag{9}$$

The Eshelby solution also gives:

$$\tau_B = \tau_2^\infty - \frac{2\mu}{(1-\nu)}\frac{b_1 b_2}{(b_1+b_2)^2}\varepsilon_B^p \tag{10}$$

where τ_2^∞ is the applied stress at infinity at reversed loading and b_1 and b_2 are the corresponding plastic zone semi-axes, which are not necessarily the same as a_1 and a_2.

Thus, the effective cyclic loading acting on the dislocation pileup line is:

$$\Delta\tau^p = \tau_A - \tau_B. \tag{11}$$

A simplified case, where $b_1 = a_1$ and $b_2 = a_2$, gives:

$$\Delta\tau^p = -\frac{\Delta\tau^\infty + 2\tau_Y(\mu/\mu_p - 1)\dfrac{1}{1-\nu}\dfrac{a_1 a_2}{(a_1+a_2)^2}}{1 + (\mu/\mu_p - 1)\dfrac{1}{1-\nu}\dfrac{a_1 a_2}{(a_1+a_2)^2}} \tag{12}$$

where $\Delta\tau^\infty = \tau_1^\infty - \tau_2^\infty$ is the applied shear stress amplitude of loading and unloading at infinity.

As expected, the plastic zone has reduced the loading acting on the dislocation pileup line, which in turn makes the fatigue life to crack initiation predicated by the above formulation longer than that obtained by Mura and Nakasone (1990). Here, some of the key equations of this model are listed.

The crack initiation cycle number is calculated based upon the change of Gibbs free energy between two states. The first state is that of dislocation dipoles piled up along two very close slip planes. The second state is the release of strain energy caused by the accumulation of dislocations by creating a micro-crack. The Gibbs free energy is

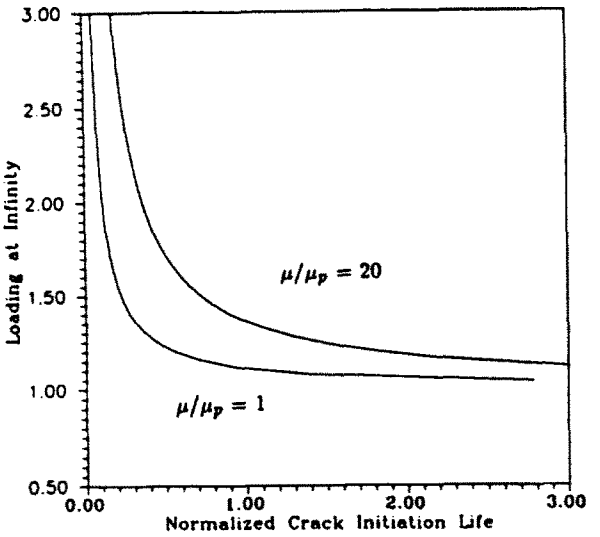

Fig. 3. $\Delta\tau^{\infty}/2\tau_f$ vs N_i.

$$\Delta G = -W_1 - W_2 + 2c\gamma \tag{13}$$

where W_1 is the strain energy of dislocation pileup and W_2 is that corresponding to an externally-loaded crack; the third term is the energy needed to create a new surface. It has been noted that W_2 is a small term when compared with W_1 when $h/a > O(10^{-4})$ (h is the height of dislocation dipole and a the pileup length) [see Fan *et al.* (1990)]. Next, a Griffith-type energy criterion is used to predict crack initiation, i.e.

$$\frac{\partial \Delta G}{\partial n} = 0$$

where n is the cycle number.

From eqn (28) of Mura and Nakasone's (1990) paper, a normalized crack initiation life can be written as:

$$N_i = \frac{2\tau_f n_i h}{\gamma} = \frac{1}{(\Delta\tau^p/2\tau_f - 1)\log(8a/h)} \tag{14}$$

where $\Delta\tau^p$ has been obtained from (12). Assuming $\tau_f = \tau_Y$,

$$N_i = \frac{1 + (\mu/\mu_p - 1)\dfrac{1}{1-\nu}\dfrac{a_1 a_2}{(a_1+a_2)^2}}{(\Delta\tau^{\infty}/2\tau_f - 1)\log(8a/h)}. \tag{15}$$

Equation (15) is drawn in Fig. 3 with $\nu = 0.3$, $a_1/a_2 = 10.0$, $h/a = 10^{-4}$ and $\tau_f = \tau_Y$. It is seen that the crack initiation is delayed by the plastic deformation surrounding the dislocation pileup layers.

3. MICRO-CRACK IN THE PLASTIC ZONE

During the early stage of the crack propagation, the as-initiated micro-crack is still partly controlled by the PSB where it has been initiated. In this stage, the effective amplitude of the stress intensity factor is reduced by the plastic deformation in the band. It is the so-called "shielding effect", although the plastic deformation is not caused by the crack itself. In the present section, this shielding effect is studied by following the eigenstrain method.

Consider the configuration described in Fig. 1(b), where a crack is in the plastic zone. When the crack size is much smaller than the plastic zone size, $c_1 \ll a_1$, the crack is also modelled as an elliptical inclusion with eigenstrain ε^c, where ε^c is determined to satisfy the traction-free condition at the crack surfaces, i.e. in Ω_c

$$\sigma^0_{12}+\sigma^*_{12}+\sigma^c_{12}=0 \quad \text{in} \quad \Omega_c \tag{16a}$$

$$\sigma^0_{22}+\sigma^*_{22}+\sigma^c_{22}=0 \quad \text{in} \quad \Omega_c \tag{16b}$$

where σ^0_{ij} is the applied stress at infinity, σ^*_{ij} is the stress disturbance caused by the plastic zone, which can be obtained from the above known ε^p, and σ^c_{ij} is caused by the crack.

Consider the pure shear loading at point A in Fig. 2, where ε^p_A is obtained in eqn (7). It is known that:

$$\sigma^*_{12} = -\frac{2\mu}{1-\nu}\frac{a_1a_2}{(a_1+a_2)^2}\varepsilon^p_A \tag{17}$$

$$\sigma^c_{12} = -\frac{2\mu}{1-\nu}\frac{c_1c_2}{(c_1+c_2)^2}\varepsilon^c_{12} \tag{18}$$

where a_1 and a_2 are the two semi-axes of the plastic zone and c_1 and c_2 are the two semi-axes of the crack; c_2 tends to zero.

For Mode II, by substituting eqns (18) and (17) into eqn (16a), with eqn (7), one may obtain:

$$\frac{2\mu}{1-\nu}\frac{c_1c_2}{(c_1+c_2)^2}\varepsilon^c_{12} = \tau^\infty_1\left(1-\frac{1}{1-\nu}\frac{a_1a_2}{(a_1+a_2)^2}\frac{1-\tau_Y/\tau^\infty_1}{\dfrac{1}{(1-\nu)}\dfrac{a_1a_2}{(a_1+a_2)^2}-\dfrac{1}{1-\mu/\mu_p}}\right) \tag{19}$$

where it is assumed that

$$\lim_{c_2\to 0} c_2\varepsilon^c_{12} = \text{finite}.$$

With these eigenstrains, the stresses at the crack tip may be calculated by considering the jump conditions across $\partial\Omega_c$ [boundary of Ω_c, $(x_1/c_1)^2+(x_2/c_2)^2=1$] as follows:

$$[\sigma_{ij}]n_j = \sigma_{ij}(\text{out})-\sigma_{ij}(\text{in})n_j = 0 \tag{20}$$

$$[u_{i,j}] = u_{i,j}(\text{out})-u_{i,j}(\text{in}) = \Lambda_i n_j \tag{21}$$

where $\mathbf{n}$ is unit normal vector of $\partial\Omega_c$ and Λ_i are to be determined. Hooke's law gives

$$[\sigma_{ij}]n_j = C_{ijkl}([u_{k,l}]-[\varepsilon^*_{kl}])n_j = 0 \tag{22}$$

where $[\varepsilon^*_{kl}] = -\varepsilon^c_{kl}$ represent jumps of the eigenstrains. With eqn (21), eqn (22) can be taken in the form of

$$C_{ijkl}\Lambda_k n_l n_j = -C_{ijkl}\varepsilon^c_{kl}n_j. \tag{23}$$

Solving eqn (23) for Λ_i, and then finding the stress jump will lead to the determination of the stress intensity factor for the crack. In order to reach this result directly, the detailed derivation of the above argument is given in Appendix B. The non-zero stress σ_{xx} on the crack surface near the crack tip is:

$$\sigma_{xx} = -2\sqrt{\frac{c_1}{2(c_1-x)}}\tau_1^{\infty}\left(1-\frac{1}{1-\nu}\frac{a_1a_2}{(a_1+a_2)^2}\frac{1-\tau_Y/\tau_1^{\infty}}{\dfrac{1}{(1-\nu)}\dfrac{a_1a_2}{(a_1+a_2)^2}-\dfrac{1}{1-\mu/\mu_p}}\right). \quad (24)$$

The shielded stress intensity factor is found from the stress expression above as:

$$\frac{K_{II}^{*}}{K_{II}^{0}} = 1-\frac{1}{1-\nu}\frac{a_1a_2}{(a_1+a_2)^2}\frac{1-\tau_Y/\tau_1^{\infty}}{\dfrac{1}{(1-\nu)}\dfrac{a_1a_2}{(a_1+a_2)^2}-\dfrac{1}{1-\mu/\mu_p}} \quad (25)$$

where

$$K_{II}^{0} = \tau^{\infty}\sqrt{\pi c_1}.$$

In the slip band model, the only non-zero plastic strain components are $\varepsilon_{12} = \varepsilon_{21}$. Thus there is no shielding on the K_I.

4. DISCUSSION

The formulations in the previous sections have modified the fatigue crack initiation model (Mura and Nakasone, 1990) and have shown micro-plastic deformation effects on the early stages of fatigue life. The calculations in Sections 2 and 3 are qualitative because the local plastic strain is approximated as a uniform distribution, and no load history is considered. Nevertheless, the effects of plastic deformation on crack initiation and micro-cracking can be estimated. The fatigue life to crack initiation, as expected, becomes a greater number as the plastic deformation is considered. A representative S–N curve with changing parameter μ/μ_p is drawn in Fig. 3, where the fatigue life to crack initiation is seen to increase as the plastic modulus decreases (Lin and Cheng, 1989). This result is consistent with the well-known fact that plastic ductility increases the fatigue life. From Fig. 4 (drawn for $\nu = 0.3$ and $a_1/a_2 = 10$), the stress intensity factor is known to be decreased by a surrounding plastic zone, and the normalized crack-tip stress intensity factor depends on the modulus of the "matrix" and "inclusion" (PSB).

It has been seen that crack shielding in our configuration does not depend on the relative crack length and the position of the crack in the inclusion and is a result of the

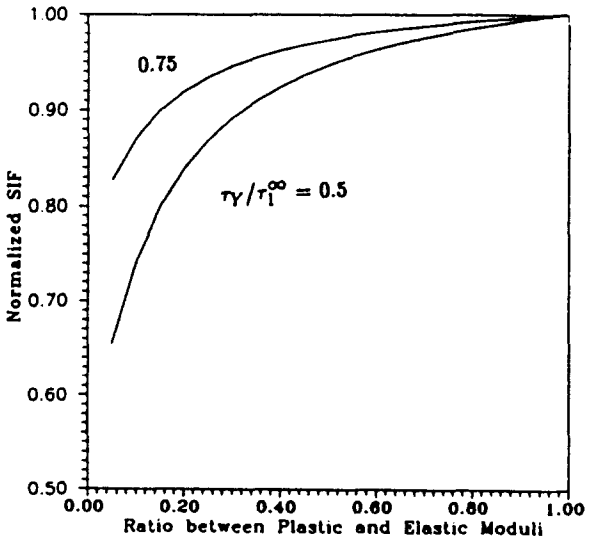

Fig. 4. K_{II}^{*}/K_{II}^{0} vs μ_p/μ.

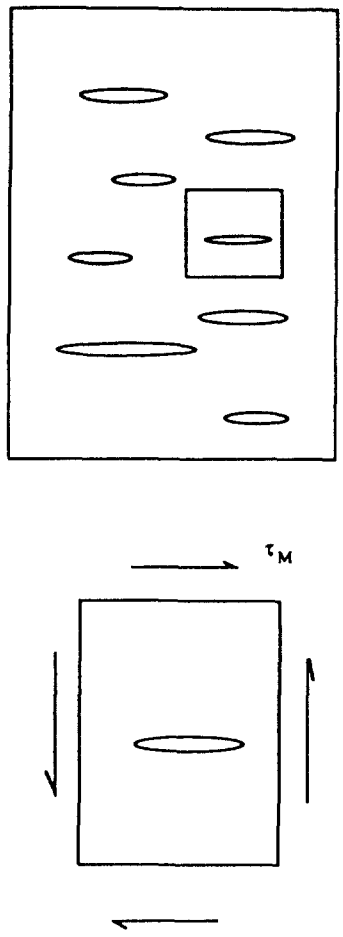

Fig. 5. A model of micro-plastic zones in fatigue.

simplification used to evaluate the eigenstrains [eqns (7) and (18)]. The eigenstrains were obtained for the plastic zone and crack separately without considering the interaction between them because $c_1 \ll a_1$. This configuration may not be close to reality for large cracks, where the relative size and position become more important. However the situation can arise, as micro-cracking in a PSB, where the crack is very small compared with the size of the damaged band. The present solution has been checked as a limit of Wu and Chen's (1990) numerical calculation.

This result is not yet suitable for comparison with experimental data, because the loading and corresponding strains have been measured for macroscopic specimens. A model which connects the macro-hysteresis loop and the micro-hysteresis loop is needed to bridge the present calculation and experimental measurements. Here, such a model, as sketched in Fig. 5 is proposed where plastic deformation measured by the macro-hysteresis loop is seen as a composition of slip in some grains which have preferred slipping systems in the direction of the macro-resolved shear stress, where the rest of the grains are assumed to be in the elastic range. Then a typical cell (Fig. 5) is a micro-plastic zone embedded in an infinite elastic body, which has been solved in the preceding sections. The loading acting on this micro-cell should be an average shear stress in the "matrix" (elastic region), which may be evaluated by using the Mori–Tanaka (Mori and Tanaka, 1973) theorem.

Acknowledgement—This research was supported by the National Science Foundation through the Contract MSM-8817869.

REFERENCES

Eshelby, J. D. (1957). The determination of the elastic field of an ellipsoidal inclusion, and related problems. *Proc. R. Soc.* **A241**, 376–396.

Essman, V., Gosele, U. and Mughrabi, H. (1981). A model of extrusion and intrusion in fatigue metals. *Phil. Mag. A.* **44**(2), 405–426.
Fan, H., Keer, L. M. and Mura, T. (1990). Near surface crack initiation under contact fatigue. Submitted to *STLE Transactions*.
Laird, C. (1978). Mechanisms and theories of fatigue. In *Fatigue and Microstructure*, pp. 149–204. ASM, Metal Park, Ohio.
Lin, M. R., Fine, M. and Mura, T. (1986). Experimental and theoretical study of fatigue crack initiation in metal. *Metall. Trans.* **34**(4), 619–628.
Lin, T. H. and Cheng, Q. Y. (1989). Introduction of slip bands in high-cycle fatigue crack initiation. In *Micromechanics and Inhomogeneity* (Edited by G. J. Weng, M. Taya and H. Abe), pp. 231–242. Springer, New York.
Mori, T. and Tanaka, K. (1973). Average stress in matrix and average energy of materials with misfitting inclusions. *Acta Metall.* **21**, 571–574.
Mura, T. (1982). *Micromechanics of Defects in Solids*. Martinus Nijhoff, The Hague.
Mura, T. and Nakasone, Y. (1990). The phenomena of fatigue crack initiation in solids. *ASME J. Appl. Mech.* March 1–7.
Ortiz, M. and Giannakopoulos, A. E. (1989). Maximal crack tip shielding by micro-crack. *ASME J. Appl. Mech.* **56**, 279–283.
Steif, P. S. (1987). A semi-infinite crack penetrated in a circular inclusion. *ASME J. Appl. Mech.* **54**, 87–92.
Tanaka, K. and Mura, T. (1981). A dislocation model for fatigue crack initiation. *ASME J. Appl. Mech.* **48**, 97–103.
Wu, C. H. and Chen, C. (1990). A crack in a confocal elliptic inhomogeneity embedded in an infinite medium. *ASME J. Appl. Mech.* **57**, 91–96.

APPENDIX A

In the present paper, an elliptical cylinder is considered (let $a_3 \to \infty$ in Eshelby's solution), where the Eshelby tensor for isotropic materials is:

$$S_{1111} = \frac{1}{2(1-\nu)}\left(\frac{a_2^2+2a_1a_2}{(a_1+a_2)^2}+(1-2\nu)\frac{a_2}{a_1+a_2}\right)$$

$$S_{2222} = \frac{1}{2(1-\nu)}\left(\frac{a_1^2+2a_1a_2}{(a_1+a_2)^2}+(1-2\nu)\frac{a_1}{a_1+a_2}\right)$$

$$S_{1122} = \frac{1}{2(1-\nu)}\left(\frac{a_2^2}{(a_1+a_2)^2}-(1-2\nu)\frac{a_2}{a_1+a_2}\right)$$

$$S_{2211} = \frac{1}{2(1-\nu)}\left(\frac{a_1^2}{(a_1+a_2)^2}-(1-2\nu)\frac{a_1}{a_1+a_2}\right)$$

$$S_{1133} = \frac{1}{2(1-\nu)}\frac{2\nu a_2}{a_1+a_2}, \quad S_{2233} = \frac{1}{2(1-\nu)}\frac{2\nu a_1}{a_1+a_2}$$

$$S_{1212} = \frac{1}{2(1-\nu)}\left(\frac{a_2^2+2a_1^2}{2(a_1+a_2)^2}+\frac{(1-2\nu)}{2}\right)$$

$$S_{2323} = \frac{a_1}{2(a_1+a_2)}, \quad S_{1313} = \frac{a_2}{2(a_1+a_2)}.$$

The remaining components are zero.

The strain caused by the eigenstrain is given by:

$$\varepsilon_{ij} = S_{ijkl}\varepsilon^*_{kl}.$$

The stress disturbance is:

$$\sigma_{ij} = C_{ijkl}(S_{klmn}\varepsilon^*_{mn} - \varepsilon^*_{kl}).$$

For isotropic materials, one may have:

$$\sigma_{12} = -\frac{2\mu}{1-\nu}\frac{a_1a_2}{(a_1+a_2)^2}\varepsilon^*_{12}.$$

APPENDIX B: STRESS INTENSITY FACTOR

Consider a crack as an elliptical cylinder with a long semi-axis c_1 in the x-direction and short semi-axis c_2 in the y-direction which will tend to be zero, i.e.:

$$\frac{x^2}{c_1^2}+\frac{y^2}{c_2^2}=1. \tag{B1}$$

The normal vector of $\partial\Omega_\varepsilon$ for a point (x, y) near the crack tip is:

$$n_1=\frac{c_2x}{\sqrt{(c_2^2x^2+c_1^4y^2/c_2^2)}}\to\frac{c_2}{\sqrt{2c_1(c_1-x)}} \tag{B2}$$

$$n_2=\frac{c_1y}{\sqrt{(c_2^4x^2/c_1^2+c_1^2y^2)}}\to 1 \tag{B3}$$

as $c_2\to 0$, $y\to 0$ and $x\to c_1$.

By substituting these values into eqn (23), one may have:

$$\Lambda_1(kn_1n_2+1)+n_1n_2k\Lambda_2=-2\varepsilon_{12}^{\infty}n_2 \tag{B4}$$

$$n_1n_2k\Lambda_1+\Lambda_2(kn_1n_2+1)=-2\varepsilon_{12}^{\infty}n_1 \tag{B5}$$

where $k=(\lambda+\mu)/\mu$.

It is noticed that the only non-zero component of stress on the crack surface is σ_{xx}, whose jump condition is given as:

$$\begin{aligned}[\sigma_{xx}]&=(\lambda+2\mu)[u_{1,1}]+\lambda[u_{2,2}]\\&=(\lambda+2\mu)\Lambda_1n_1+\lambda\Lambda_2n_2.\end{aligned} \tag{B6}$$

By substituting the solutions of Λ_1 and Λ_2, which have been solved from (B4) and (B5),

$$\sigma_{xx}=[\sigma_{xx}]=-\frac{2\mu}{1-\nu}2\varepsilon_{12}^{\infty}n_1. \tag{B7}$$

By using the limit (B2) and $\varepsilon_{12}^{\infty}c_2=$ finite, with $\varepsilon_{12}^{\infty}$ in eqn (19), one may obtain:

$$\sigma_{xx}=-2\sqrt{\frac{c_1}{2(c_1-x)}}\tau_1^{\infty}\left(1-\frac{1}{1-\nu}\frac{a_1a_2}{(a_1+a_2)^2}\frac{1-\tau_Y/\tau_1^{\infty}}{1}\frac{a_1a_2}{(1-\nu)}\frac{1}{(a_1+a_2)^2}\frac{1}{1-\mu/\mu_p}\right). \tag{B8}$$